



# Understanding the Behaviour of Real Metaborates in Solution

Frances Pope,<sup>[a]</sup> Noë I. Watson,<sup>[a]</sup> Antoine Deblais,<sup>[b]</sup> and Gadi Rothenberg\*<sup>[a]</sup>

Alkali metal borohydrides are promising candidates for large-scale hydrogen storage. They react spontaneously with water, generating dihydrogen and metaborate salts. While sodium borohydride is the most studied, potassium has the best chance of commercial application. Here we examine the physical and chemical properties of such self-hydrolysis solutions. We do this by following the hydrogen evolution, the pH changes, and monitoring the reaction intermediates using NMR. Most studies on such systems are done using dilute solutions, but real-life applications require high

concentrations. We show that increasing the borohydride concentration radically changes the system's microstructure and rheology. The changes are seen already at concentrations as low as 5 w/w%, and are critical above 10 w/w%. While dilute solutions are Newtonian, concentrated reaction solutions display non-Newtonian behaviour, that we attribute to the formation and (dis)entanglement of metaborate oligomers. The implications of these findings towards using borohydride salts for hydrogen storage are discussed.

## Introduction

Drastic climate changes are driving research towards green energy sources and cycles. Two sectors that are especially crucial in this respect are transportation and mobile power generation. These sectors account for over 22% of CO<sub>2</sub> emission equivalents worldwide.<sup>[1]</sup> The best way to deal with this problem is by using carbon-free fuels, eliminating CO<sub>2</sub> emissions and reducing air pollution.<sup>[2]</sup> Part of the transportation sector is moving towards battery power, but heavy vehicles, boats and mobile generators require other solutions.<sup>[3,4]</sup> Of these, hydrogen is the most promising alternative.

Hydrogen can be stored as compressed gas, as a liquid, or bound to a liquid or a solid carrier.<sup>[5]</sup> Each option has its own problems. Compressed hydrogen gas and liquefied hydrogen both require extreme conditions (high pressures and low temperatures).<sup>[6]</sup> This makes them inefficient and dangerous for large-scale operations. Chemical storage of hydrogen in liquid organic carriers (LOHCs) are easily manageable and transportable.<sup>[7]</sup> However, they require high heat and precious metal catalysts to release the hydrogen.<sup>[8,9]</sup> Similarly, storage as inorganic salts adds dead weight to the fuel.

Yet of all these methods, the latter has the advantages of safe long-term storage and transportation. This is especially

true in the case of metal borohydrides.<sup>[10,11]</sup> These solids can be stored safely at room temperature and ambient pressure. They have a high hydrogen density by weight.<sup>[12]</sup> Moreover, the high chemical energy stored in the boron-hydrogen bonds allows them to react spontaneously with water, giving four molecules of hydrogen per borohydride ion, with the corresponding metaborate salt as a side-product (eq 1). The metaborate is formed by the decomposition of tetrahydroxyborate, which is the initial product of the borohydride hydrolysis. Metaborates occur in various hydrated forms, depending on the reaction conditions.<sup>[13]</sup> For controlled hydrogen release, which is preferable for real-life applications, the spontaneous (slow) dehydrogenation can be suppressed by adding hydroxide ions.<sup>[14]</sup> This reaction, although spontaneous, is slow and can be accelerated by adding a catalyst.



A significant limitation in the use of borohydrides has been the regeneration of the starting material from the metaborate product. This is a costly and energy intensive process, resulted in 2007 in a no-go recommendation for NaBH<sub>4</sub> from the US Department of Energy.<sup>[15]</sup> However, in the past 15 years there have been significant steps in the energy and economical efficiency of this regeneration.<sup>[16–18]</sup> These developments are resetting borohydride technology as an effective hydrogen energy storage option.

Owing to its low price, general availability and high hydrogen density (10.7 wt%), NaBH<sub>4</sub> is the most popular borohydride candidate for hydrogen storage.<sup>[12]</sup> Yet it has one inherent disadvantage: its product, sodium metaborate, dissolves poorly in water (0.28 g/mL at 25 °C).<sup>[19]</sup> This low solubility causes crystallisation in piping and machinery, barring many real-life applications.<sup>[15]</sup> As this solubility is a thermodynamic constraint, it cannot be circumvented easily. Instead, potassium borohydride (KBH<sub>4</sub>, containing 7.5 wt% hydrogen) could be a viable alternative, as the solubility of potassium metaborate in water is

[a] F. Pope, N. I. Watson, Prof. Dr. G. Rothenberg  
Van't Hoff Institute for Molecular Sciences  
University of Amsterdam  
Science Park 904, 1098 XH Amsterdam, The Netherlands  
E-mail: g.rothenberg@uva.nl  
Homepage: <http://hims.uva.nl/hcsc>

[b] Dr. A. Deblais  
Institute of Physics  
University of Amsterdam  
Science Park 904, 1098 XH Amsterdam, The Netherlands

© 2022 The Authors. ChemPhysChem published by Wiley-VCH GmbH. This is an open access article under the terms of the Creative Commons Attribution Non-Commercial License, which permits use, distribution and reproduction in any medium, provided the original work is properly cited and is not used for commercial purposes.

much higher (the literature reports 1.51 g/mL at 25 °C,<sup>[20,21]</sup> while our own measurements show up to 1.75 g/mL).

The problem is that we know little about the behaviour of borohydride/metaborate mixtures in concentrated solutions. This is important, because there is a marked difference between dilute and concentrated solutions of these salts. Published studies on borohydrides and metaborates often use dilute (and therefore homogeneous) solutions.<sup>[22–24]</sup> In such cases, a direct comparison between the dehydrogenation of NaBH<sub>4</sub> and KBH<sub>4</sub> is reasonable. But dilute solutions are impractical in many real-life fuel applications, because the excess water is mere ballast. In theory, a 2:1 stoichiometric ratio of water to borohydride would be ideal, but this does not allow for the solubility of the reactants and products. Some excess water must be used, creating a trade-off between the desire for high energy density (concentrated fuel) and workability (enough water to solubilise the reactants and products). In concentrated solutions, the comparison between the sodium and potassium systems no longer holds, because of the difference in solubilities of both borohydrides and metaborates. This means that any conclusions regarding the performance of potassium borohydride as fuel must be based on independent studies of potassium borohydride systems.

Addressing this problem, we study here the self-hydrolysis and rheology behaviour of dilute and concentrated KBH<sub>4</sub> solutions under a variety of laboratory and simulated industrial conditions. Our results show that the properties of concentrated solutions significantly differ from those of dilute ones. This gives insight into the intermediates formed during self-hydrolysis at these higher concentrations.

## Results and Discussion

We began by studying the spontaneous self-hydrolysis of KBH<sub>4</sub>. Often, for catalysis-driven fuel applications, the borohydride solutions are stabilised with hydroxide salts.<sup>[25]</sup> This suppresses the spontaneous dehydrogenation, preventing fuel loss and giving control over the reaction kinetics when a catalyst is added. However, studying the non-stabilised fuel can tell us much about the products that form in this reaction system.

In a typical set of experiments, we tested the self-hydrolysis of KBH<sub>4</sub> at concentrations ranging from 0.1 to 20 w/w%. The reactions were monitored on-line using either a high-precision bubble counter (for the low concentrations) or a flow meter (for the higher concentrations, see experimental section for details).<sup>[26]</sup> Using higher KBH<sub>4</sub> concentrations gave higher initial hydrogen generation rates, yet resulted in overall lower percentage H<sub>2</sub> yields (Table 1). For example, the self-hydrolysis of 5 w/w% KBH<sub>4</sub> produced a 92% yield (1.45 L H<sub>2</sub>) over 13 h at 65 °C, while 20 w/w% produced a 47% yield (2.95 L H<sub>2</sub>) in the same time frame.

Looking at Figure 1, we see that the rate of hydrogen evolution decreased over time for all self-hydrolysis reactions. This agrees with the results of Sahin et al. where 20 w/w% KBH<sub>4</sub> gave 50% hydrogen yield after 240 min at 60 °C, with decreasing hydrogen production over time.<sup>[27]</sup> Simultaneously, the pH increased, decreasing H<sub>2</sub> production.<sup>[14]</sup> These reactions were monitored online with continuous pH measurements. We

**Table 1.** Hydrogen yields and pH of self-hydrolysis of KBH<sub>4</sub> solutions at a range of concentrations, and the pH of their equivalent KBO<sub>2</sub> concentrations.<sup>[a]</sup>

Entry	KBH <sub>4</sub> [w/w%]	H <sub>2</sub> yield [%]	Volume [L]	Final pH of self-hydrolysis soln	pH of equiv. KBO <sub>2</sub> soln
1 <sup>[b]</sup>	0.1	103 <sup>[d]</sup>	0.03	10.50	10.94
2 <sup>[c]</sup>	5	92	1.45	12.30	12.44
3 <sup>[c]</sup>	10	80	2.51	13.06	13.11
4 <sup>[c]</sup>	20	63	3.95	13.99	13.91

<sup>[a]</sup> Reaction conditions: 15 mL deionised water, 65 °C, magnetic stirring at 250 rpm. All results are averages of duplicate experiments. <sup>[b]</sup> Hydrogen generation measured using a high-precision bubble counter. <sup>[c]</sup> Hydrogen generation measured using a mass flow meter. <sup>[d]</sup> value is within margin of error of mass balance.

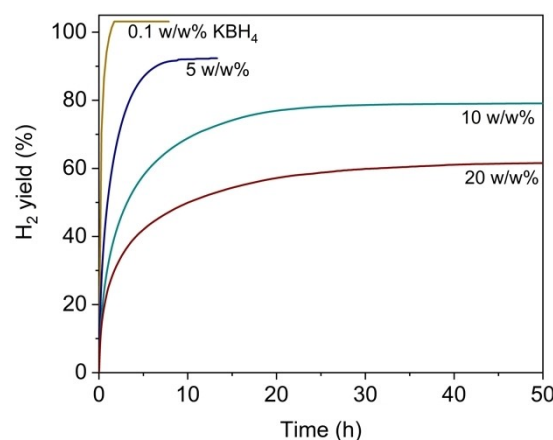


**Figure 1.** H<sub>2</sub> yield of self-hydrolysis of KBH<sub>4</sub> at concentrations from 0.1–20 w/w% in H<sub>2</sub>O at 65 °C. Plots are based on mass flow meter measurements taken once per second.

attribute the decreasing rate of self-hydrolysis to the increasing pH. We also ran the same reactions in the presence of a buffer. However, all protons were consumed, and H<sub>2</sub> generated, so the pH could not be maintained.

In a set of control experiments, we then compared the final pH values of the completed self-hydrolysis reactions to those of solutions containing the equivalent concentrations of pure KBO<sub>2</sub> (Table 1, all other conditions were identical). The similar pH values show that the basicity results from the KBO<sub>2</sub> product, rather than from the self-hydrolysis reaction (the pK<sub>a</sub> of boric acid, HBO<sub>2</sub>, is 9.15). This is important, as it shows that the self-hydrolysis of concentrated KBH<sub>4</sub> solutions is self-limiting in the absence of a catalyst.

To further confirm the influence of pH on the self-hydrolysis reaction, KOH was added to 5 w/w% KBH<sub>4</sub> solutions, drastically increasing the pH of the starting solution. This diminished the self-hydrolysis significantly. In fact, when 5 w/w% KOH was added, only 564 mL (equivalent to 40% yield) H<sub>2</sub> gas was released over 7 days, compared to 1.45 L (92% yield) in 13.3 h with no KOH (Figure 2). Another control experiment confirmed that adding 1 w/w% KOH to the 5 w/w% KBH<sub>4</sub> solution increased the pH significantly enough to suppress hydrogen generation even at 65 °C, generating only 384 mL H<sub>2</sub> (24% yield) in 24 h.

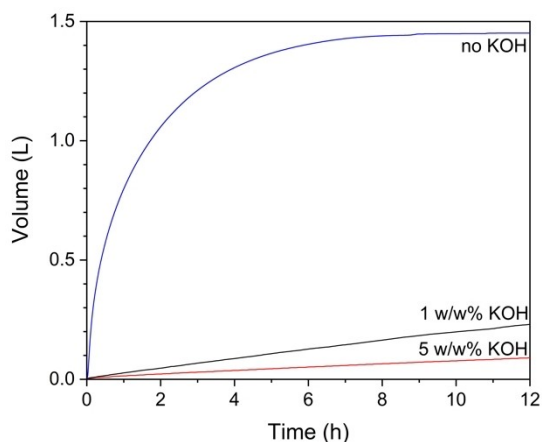


**Figure 2.**  $\text{H}_2$  yield is suppressed by alkaline conditions. 1 and 5 w/w% KOH were added to 5 w/w%  $\text{KBH}_4$  self-hydrolysis solutions at  $65^\circ\text{C}$ . Plots are based on mass flow meter measurements taken once per second.

We can learn more about these reactions from rheological studies. As expected, different reaction solutions showed different starting viscosities. During the reaction, however, the viscosity also changed, increasing with the reaction progress. This change in viscosity was much more pronounced for more concentrated  $\text{KBH}_4$  solutions. We measured the hydrolysis solutions at concentrations of 1, 5, 10 and 20 w/w%  $\text{KBH}_4$ . The samples were measured under a range of applied flows (so-called shear rates). Interestingly, some of the “end-of-reaction” solutions were not only highly viscous, but also showed different shear behaviour compared to water. Water maintains its viscosity regardless of the shear rate. This is known as Newtonian behaviour.<sup>[28]</sup> At 1 w/w%  $\text{KBH}_4$ , the self-hydrolysis product solutions showed a constant viscosity under changing shear rates from 1 to  $1000\text{ s}^{-1}$ , confirming this Newtonian behaviour (Figure 3). This can be related to the micro-

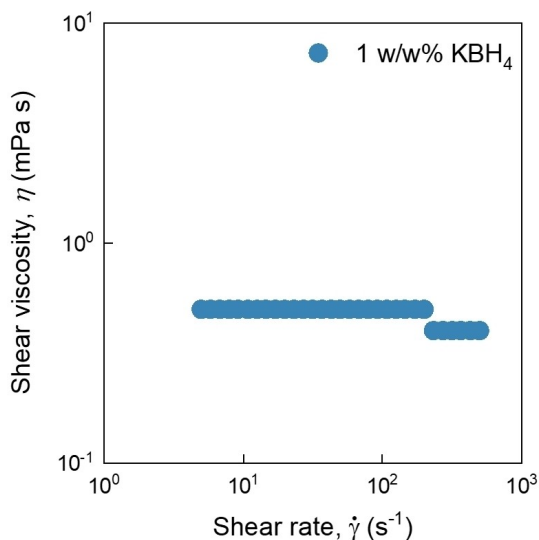


**Figure 3.** Rheology of fully hydrolysed 1 w/w%  $\text{KBH}_4$  solution showing Newtonian fluid behaviour (the slight change in the viscosity seen at higher shear rates is within the experimental error margin).

structure of the solution.<sup>[29]</sup> If applying a force to the solution has no effect on its viscosity, it does not affect the solution microstructure. We can thus view these dilute solutions as a collection of homogeneous, weakly interacting species in water.

However, at concentrations of 5 w/w%  $\text{KBH}_4$  and above, the rheology measurements showed a change in viscosity over time, with shear thinning in the range from  $1\text{ s}^{-1}$  to  $1000\text{ s}^{-1}$  (see experimental section for details). This confirmed that the spent self-hydrolysis solution was non-Newtonian: Increasing the shear rate caused a rearrangement in its microstructure (Figure 4).<sup>[28]</sup>

To determine the reversibility of this change, we first increased and then decreased the shear rate. A fluid with a fully reversible pathway via the exact inverted path would indicate a microstructure that can rearrange and then return to its original state via the same route.<sup>[30]</sup> For example, agglomerations of spherical molecules can be dispersed evenly due to their weak intermolecular interactions when force is applied. Then, when the force is decreased, the molecules can begin to agglomerate again. However, a fluid that does not undergo a reversible, exactly inverted pathway indicates a more complex route. For example, non-spherical particles could align in the direction of applied force. Once this force is removed, the particles are no longer aligned by force, but cannot return to their exact previous state. Furthermore, if the pathway is not fully reversible, more permanent changes in structure, such as disentanglement of polymers, may occur.<sup>[31–34]</sup>

The 5 w/w% solution showed that the viscosity reduction was reversible, albeit that the shear thinning proceeded by shear thickening followed different pathways. This implies a more complex microstructure rearrangement than just simple dispersion and agglomeration of spherical particles. However, due to the reversibility of the shear thinning at this concentration, we propose that non-spherical particles, comprised of oligomers of metaborate with weak intermolecular reactions,

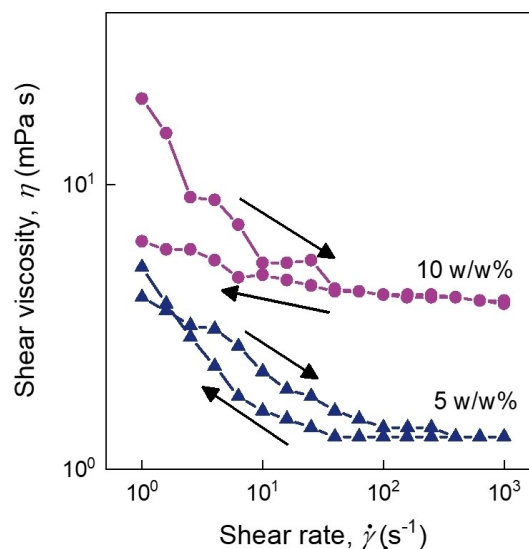
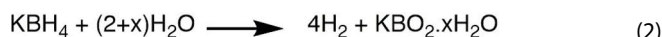


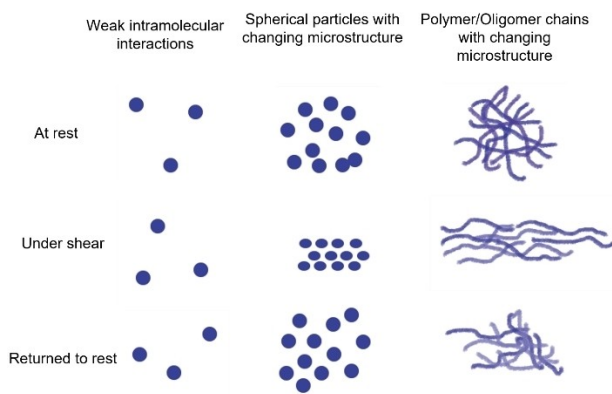
**Figure 4.** Rheology of self-hydrolysed 5 and 10 w/w%  $\text{KBH}_4$  solutions showing non-Newtonian fluid behaviour. Arrows show the shear thinning followed by shear thickening of the solutions.

were formed. At the higher concentration of 10 w/w%, the viscosity reduction of the solution was no longer reversible, showing that more complex microstructures are formed. We attribute this behaviour at higher concentrations to the disentanglement of metaborate oligomers (Scheme 1).<sup>[35]</sup>

We then ran a set of control experiments to determine if this changing viscosity was also seen in pure, off-the-shelf metaborate solutions (all samples were measured under identical conditions, see experimental section for details). For these controls, we used the equivalent amount of  $\text{KBO}_2$  that would be generated by full conversion of  $\text{KBH}_4$  in water according to eq 2.



At concentrations of 5 w/w% equivalent  $\text{KBO}_2$  we observed a fully reversible shear thinning, which is common for aggregate particles under shear. Unlike the self-hydrolysis solution, this



**Scheme 1.** Schematic representation of how three different microstructures (weakly interacting molecules, spherical particles and oligomer structures) are effected by increase then decrease in shear.

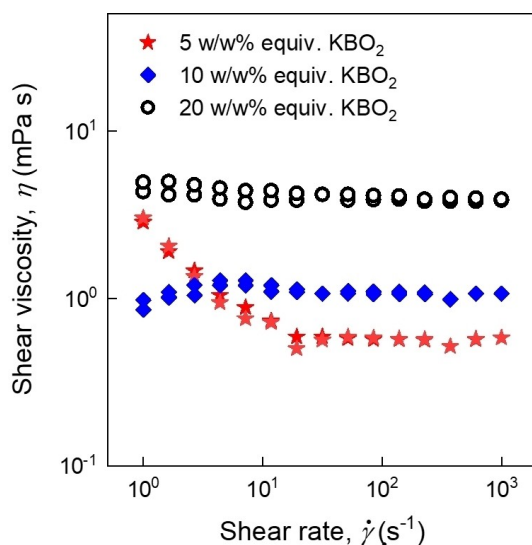


**Figure 5.** Rheology of pure  $\text{KBO}_2$  in  $\text{H}_2\text{O}$  at concentrations of 5, 10 and 20 w/w% equivalence.

thinning and thickening followed the same pathway both ways. This confirms that the microstructure of the self-hydrolysis solution is more complex than that of pure  $\text{KBO}_2$  in water.

At high concentrations of equivalent pure metaborate (10 w/w% and 20 w/w% equivalent  $\text{KBO}_2$ ), the viscosity remained constant regardless of the change in shear rate (Figure 5). This shows a homogeneous mixture with no complex microstructure changes. Importantly, this differs from the non-Newtonian behaviour of the self-hydrolysis solutions. This difference was especially prominent in the case of the 10 w/w% (Figure 6). For this concentration, the self-hydrolysis solution acted as a disentangled polymer or oligomer. Additionally, with only 80%  $\text{H}_2$  yield, we did not get full conversion to  $\text{KBO}_2$ , so this mixture also contained other reaction intermediates. We conclude that at high concentrations self-hydrolysis solutions are not comparable to pure  $\text{KBO}_2$  solutions. This is further supported by the complex microstructure deduced from the rheology measurements. Indeed, X-ray diffraction patterns of the dried product did not match those of pure  $\text{KBO}_2$ .

We can gain further insight into the species in this system by considering the reaction pathway (Scheme 2). The overall reaction shown in eq 2 above, consists of several redox steps that occur simultaneously.<sup>[36]</sup> We obtained experimental proof of the first step from NMR experiments using  $\text{KBH}_4$  powder in  $\text{D}_2\text{O}$ . The spectra clearly show the formation of the  $\text{KBH}_3\text{OH}$  intermediate (Figure 7), in agreement with published results<sup>[34]</sup> (running  $^{11}\text{B}$  NMR did not give any additional information). Although we could not observe the following steps with NMR, due to the simultaneous nature of the reaction, there is no reason to suppose that the hydrides follow a different pathway. The abstraction of the first hydride from  $\text{KBH}_4$  is thought to be the rate-determining step.<sup>[37]</sup> All of the borohydride ions react with water, and the degree of conversion depends on the time and the reaction conditions. The fact that the hydrogen yield decreases when the reaction is run at higher

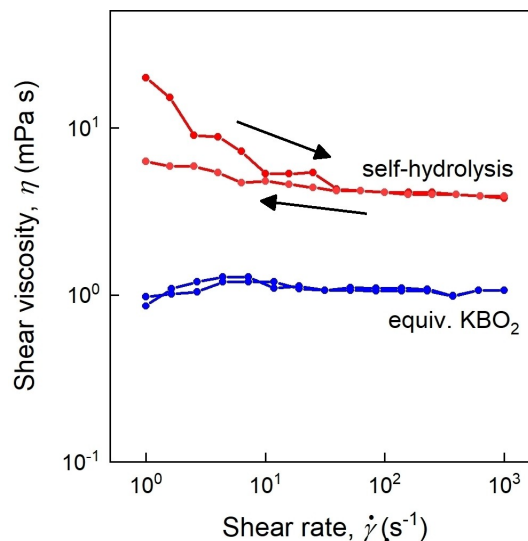
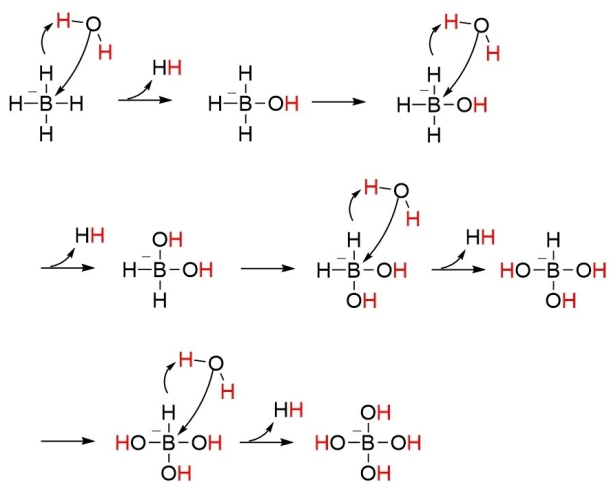


**Figure 6.** Rheology of 10 w/w%  $\text{KBH}_4$  self-hydrolysis solution vs the equivalent  $\text{KBO}_2$  in solution.



**Scheme 2.** Simplified self-hydrolysis pathway assuming individual molecule formation with no complex structures forming.

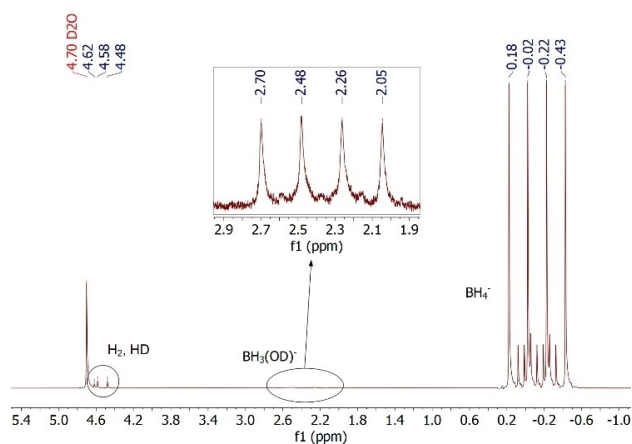


**Figure 7.**  $^1\text{H}$  NMR of self-hydrolysis of  $\text{KBH}_4$  in  $\text{D}_2\text{O}$  shows the formation of the first intermediate,  $\text{KBH}_3\text{OH}$ .

concentrations reflects the formation of these complex metabolite intermediates.

## Conclusions

$\text{KBH}_4$  hydrolysis differs from that of  $\text{NaBH}_4$  due to the difference in solubility of the corresponding metaborate salts. In theory,  $\text{KBH}_4$  is a promising hydrogen storage medium. In practice, however, high concentrations are needed for economically viable real-life applications. This matters, because dilute and concentrated solutions are not equivalent and act differently. Above 5 w/w%,  $\text{KBH}_4$  self-hydrolysis leads to the formation of complex microstructures, resulting in non-Newtonian behaviour under change in shear. In addition, at higher concentrations, the irreversible microstructure rearrangement under shear show polymer-like properties. We attribute these to the (dis)entanglement of metaborate oligomers. Furthermore, we show that spent  $\text{KBH}_4$

reaction solutions differ from pure  $\text{KBO}_2$  solutions in these properties. Overall, our results show that moving to industrially relevant concentrations changes the products' properties. Not only are the physical properties of the product solution non-Newtonian, but complex oligomer intermediates form as a result.

## Experimental Section

**Materials and instrumentation.** Hydrogen generation was measured on a high-precision bubble counter constructed in-house<sup>[26]</sup> or a Bronkhorst EL-Flow Prestige mass flow meter with a maximum 150 mL/min flow rate (normalised to  $\text{H}_2$ ). In situ and end-of-reaction pH measurements were taken using a Eutech Instruments PC 2700 pH meter. The rheological measurements were performed with a stress-controlled rheometer (Anton Paar MCR 302). A 50 mm-diameter cone-and-plate geometry was used with a  $1^\circ$  cone. The experiments were performed at a gap size of 0.101  $\mu\text{m}$  and at a temperature of  $65^\circ\text{C}$  set by a Peltier system (Anton Paar, measurement cell P-PTD200/AIR).  $^1\text{H}$  spectra were recorded on a Bruker AV 500NEO NMR spectrometer using  $\text{D}_2\text{O}$  as a solvent. Powder XRD was measured on a MiniFlex II diffractometer with  $\text{Cu K}\alpha$  at 30 kV and 14 mA. Patterns were recorded between  $5^\circ$  and  $90^\circ$  with a rate of  $2.5^\circ/\text{min}$ .  $\text{KBH}_4$  (98%),  $\text{KOH}$  (85%) and  $\text{KBO}_2 \cdot x\text{H}_2\text{O}$  (99+%) were bought from Alfa Aesar.  $\text{D}_2\text{O}$  was bought from Sigma Aldrich. All materials were used as received. We used  $\text{KBH}_4$  concentrations of 0.1–20 w/w%, where w/w% denotes the % of the weight of water used. For example, a 5 w/w% solution would contain 5 g of  $\text{KBH}_4$  in 100 g of water.

**General procedure for dehydrogenation experiments.**  $\text{KBH}_4$  was put in a round bottom flask and placed in an oil bath. 15 mL  $\text{H}_2\text{O}$  was heated to  $65^\circ\text{C}$  and transferred to a dropping funnel attached to the RBF. The glassware was flushed with air, then the water was dropped into the RBF and  $\text{H}_2$  measurements were immediately started.  $\text{H}_2$  was measured on a flow meter.

**Example: dehydrogenation of 5 w/w%  $\text{KBH}_4$ .** 0.77 g (14.28 mmol, 5 w/w%)  $\text{KBH}_4$  was put in to a round bottom flask with a stir bar and placed in an oil bath. 15 mL of  $65^\circ\text{C}$   $\text{H}_2\text{O}$  was put in a dropping funnel attached to the RBF. The closed set-up with connected to a cold trap in an ice bath and then attached to a flow meter. The reactor was flushed with 60 mL air using a syringe and needle into the closed system. Once the system had been flushed, the water was dropped into the round bottom flask and  $\text{H}_2$  measurements were taken.

For  $\text{KBO}_2$  equivalent measurements, the molar equivalent of  $\text{KBO}_2$  to initial  $\text{KBH}_4$  was measured. This was added to  $\text{H}_2\text{O}$ , taking into consideration  $\text{H}_2\text{O}$  that would have been consumed during the reaction. This mixture was left to stir at  $65^\circ\text{C}$  to ensure the same conditions for rheology measurements.

**Procedure for rheological measurements.** Samples were first heated to  $65^\circ\text{C}$  and kept at this temperature for 1000 s, while the shear viscosity was measured at a constant and low shear rate of  $1 \text{ s}^{-1}$ . A homemade humidity chamber around the measuring plate (so-called 'geometry') was continuously flushed with humid air (80%) and allowed us to suppress evaporation during the whole measurement (a 3D-printed humidity chamber around the geometry suppresses evaporation during the measurement time. The humidity rate inside the chamber is controlled with an Arduino<sup>®</sup>; a feedback loop allows to flush the chamber with the right amount of dry/humid air). During this period, measurement of the shear viscosity allowed us to check that the samples was not subject to evaporation and that the samples were correctly thermalised. Once the equilibrium was reached, steady shear measurements were performed using increasing shear rate sweeps from 1 to  $1000 \text{ s}^{-1}$ , followed by a decreasing ramp from 1000 to  $1 \text{ s}^{-1}$  over 250 s (see Figure 8).

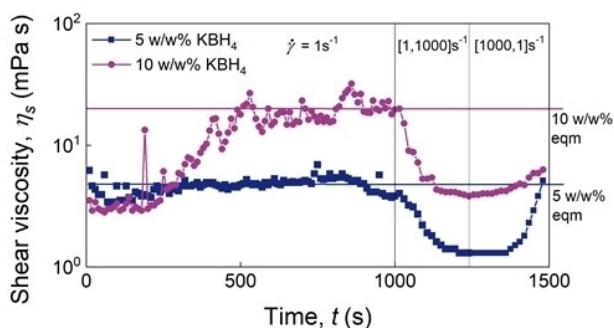


**Figure 8.** The first 1000 s of each rheology measurement was used for heating of the solution to temperature, then allowing the solution to reach equilibrium (eqm) under constant shear. During the first 1000 seconds, the solution is out of equilibrium, hence the fluctuations in viscosity.

For the self-hydrolysis viscosity measurements, a 1–2 mL sample was taken directly from the completed reaction mixture. For KBO<sub>2</sub> equivalent measurements, the molar equivalent KBO<sub>2</sub> and reduced water content was calculated. The KBO<sub>2</sub> was dissolved in the calculated reduced water and stirred overnight at 65 °C. Then, rheological measurements were taken.

NMR experiments were run following a modification of the procedure published by Demirci and co-workers.<sup>[38]</sup> Samples were prepared by adding 1 mL D<sub>2</sub>O to 36 mg KBH<sub>4</sub> (1.50 mmol, 3.5 w/w%) in a high pressure NMR tube. Spectra were taken every 30 min for 300 min.

## Acknowledgements

This work was funded by the “Austrian COMET-Program” (project InTribology1, no. 872176) via the Austrian Research Promotion Agency (FFG) and the federal states of Niederösterreich and Vorarlberg and has been carried out within the “Excellence Centre of Tribology” (AC2T research GmbH). We thank the research team of Electriq ~ Global for support and discussions.

## Conflict of Interest

The authors declare no conflict of interest.

## Data Availability Statement

The data that support the findings of this study are available from the corresponding author upon reasonable request.

**Keywords:** dehydrogenation · self-hydrolysis · rheology · potassium borohydride · hydrogen storage

[1] C. Kern, A. Jess, *Energies* **2021**, *14*, 5260.

[2] C. D. Koolen, G. Rothenberg, *ChemSusChem* **2019**, *12*, 164–172.

[3] M. Muratori, T. Mai, *Environ. Res. Lett.* **2020**, *16*, 011003.

- [4] A. Masias, in *Behaviour of Lithium-Ion Batteries in Electric Vehicles: Battery Health, Performance, Safety, and Cost* (Eds.: G. Pistoia, B. Liaw), Springer International Publishing, Cham, **2018**, pp. 1–33.
- [5] J. O. Abe, A. P. I. Popoola, E. Ajenifuja, O. M. Popoola, *Int. J. Hydrogen Energy* **2019**, *44*, 15072–15086.
- [6] T. Q. Hua, R. K. Ahluwalia, J.-K. Peng, M. Kromer, S. Lasher, K. McKenney, K. Law, J. Sinha, *Int. J. Hydrogen Energy* **2011**, *36*, 3037–3049.
- [7] P. Preuster, C. Papp, P. Wasserscheid, *Acc. Chem. Res.* **2017**, *50*, 74–85.
- [8] D. Teichmann, W. Arlt, P. Wasserscheid, *Int. J. Hydrogen Energy* **2012**, *37*, 18118–18132.
- [9] D. Teichmann, W. Arlt, P. Wasserscheid, R. Freymann, *Energy Environ. Sci.* **2011**, *4*, 2767–2773.
- [10] J. M. Hanlon, H. Reardon, N. Tapia-Ruiz, D. H. Gregory, *Aust. J. Chem.* **2012**, *65*, 656–671.
- [11] J. Andersson, S. Grönkvist, *Int. J. Hydrogen Energy* **2019**, *44*, 11901–11919.
- [12] L. Laversenne, C. Goutaudier, R. Chiriach, C. Sigala, B. Bonnetot, *J. Therm. Anal. Calorim.* **2008**, *94*, 785–790.
- [13] A. V. Churikov, K. V. Zapsis, V. V. Khramkov, M. A. Churikov, I. M. Gamayunova, *J. Chem. Eng. Data* **2011**, *56*, 383–389.
- [14] V. G. Minkina, S. I. Shabunya, V. I. Kalinin, V. V. Martynenko, A. L. Smirnova, *Int. J. Hydrogen Energy* **2012**, *37*, 3313–3318.
- [15] U. S. Department of Energy Independent Review, *Go No-Go Recommendation for Sodium Borohydride for On-Board Vehicular Hydrogen Storage*, **2007**, NREL/MP-150-42220.
- [16] L. Ouyang, W. Chen, J. Liu, M. Felderhoff, H. Wang, M. Zhu, *Adv. Energy Mater.* **2017**, *7*, 1700299.
- [17] K. Chen, L. Ouyang, H. Zhong, J. Liu, H. Wang, H. Shao, Y. Zhang, M. Zhu, *Green Chem.* **2019**, *21*, 4380–4387.
- [18] Y. Zhu, L. Ouyang, H. Zhong, J. Liu, H. Wang, H. Shao, Z. Huang, M. Zhu, *Angew. Chem. Int. Ed.* **2020**, *59*, 8623–8629; *Angew. Chem.* **2020**, *132*, 8701–8707.
- [19] N. P. Nies, R. W. Hulbert, *J. Chem. Eng. Data* **1967**, *12*, 303–313.
- [20] O. Krol, J. Andrieux, J. J. Counieux, R. Tenu, C. Goutaudier, in *XXXV JEEP – 35th Conference on Phase Equilibria*, EDP Sciences, Annecy, France, **2009**, p. 00023. DOI: 10.1051/jeeep/200900023.
- [21] P. Toledano, *Compt. Rend. Acad. Sci.* **1962**, *254*, 2348–2350.
- [22] D. Kilinc, O. Sahin, *Renewable Energy* **2020**, *161*, 257–264.
- [23] Y.-J. Lee, A. Badakhsh, D. Min, Y. S. Jo, H. Sohn, C. W. Yoon, H. Jeong, Y. Kim, K.-B. Kim, S. W. Nam, *Appl. Surf. Sci.* **2021**, *554*, 149530.
- [24] Y. Wei, M. Wang, W. Fu, L. Wei, X. Zhao, X. Zhou, M. Ni, H. Wang, *J. Alloys Compd.* **2020**, *836*, 155429.
- [25] Y. Shang, R. Chen, *Energy Fuels* **2006**, *20*, 2142–2148.
- [26] T. K. Slot, N. R. Shiju, G. Rothenberg, *Angew. Chem. Int. Ed.* **2019**, *58*, 17273–17276; *Angew. Chem.* **2019**, *131*, 17433–17436.
- [27] O. Sahin, H. Dolas, M. Ozdemir, *Int. J. Hydrogen Energy* **2007**, *32*, 2330–2336.
- [28] F. Irgens, in *Rheology and Non-Newtonian Fluids* (Ed.: F. Irgens), Springer International Publishing, Cham, **2014**, pp. 1–16.
- [29] R. I. Tanner, *Engineering Rheology*, OUP Oxford, **2000**.
- [30] R. P. Chhabra, in *Rheology of Complex Fluids* (Eds.: J. M. Krishnan, A. P. Deshpande, P. B. S. Kumar), Springer, New York, NY, **2010**, pp. 3–34.
- [31] J. Mewis, N. J. Wagner, *Adv. Colloid Interface Sci.* **2009**, *147–148*, 214–227.
- [32] P. H. S. Santos, M. A. Carignano, O. Campanella, *Gels* **2017**, *3*, 45.
- [33] J. M. Maerker, S. W. Sinton, *J. Rheol.* **1998**, *30*, 77.
- [34] L. A. Archer, *J. Rheol.* **1999**, *43*, 1617–1633.
- [35] F. Y. Zhu, C. H. Fang, Y. Fang, Y. Q. Zhou, H. W. Ge, H. Y. Liu, *J. Mol. Struct.* **2014**, *1070*, 80–85.
- [36] T. Mondal, A. Sermiagin, D. Meyerstein, T. Zidki, H. Kornweitz, *Nanoscale* **2020**, *12*, 1657–1672.
- [37] Y. Zhou, C. Fang, Y. Fang, F. Zhu, H. Liu, H. Ge, *Int. J. Hydrogen Energy* **2016**, *41*, 22668–22676.
- [38] J. Andrieux, U. B. Demirci, J. Hannauer, C. Gervais, C. Goutaudier, P. Miele, *Int. J. Hydrogen Energy* **2011**, *36*, 224–233.

Manuscript received: June 21, 2022

Revised manuscript received: July 14, 2022

Version of record online: September 7, 2022